COMPARATIVE VISIBILITY OF PLANETARY AURORAL RADIO EMISSIONS AND IMPLICATIONS FOR THE SEARCH FOR EXOPLANETS

L. Lamy[1,2*], J. E. Waters[1], and C. K. Louis[3]

*Corresponding author: laurent.lamy@obspm.fr

Citation:

Lamy et al., 2023, Comparative visibility of planetary auroral radio emissions and implications for the search for exoplanets, *in Planetary, Solar and Heliospheric Radio Emissions IX, edited by C. K. Louis, C. M. Jackman, G. Fischer, A. H. Sulaiman, P. Zucca, published by DIAS, TCD*, pp. 469–483, doi: 10.25546/103091

Abstract

The auroral regions of the so-called radio planets are the source of powerful, non-thermal, radio emissions amplified by an electron-wave resonant instability. These emissions are produced near the planetary magnetic poles along high latitude magnetic flux tubes at altitudes ranging from above the atmosphere up to a few planetary radii, and over variable ranges of local time and longitude. The radiated waves are also beamed at large angles from the local magnetic field vector, along a hollow cone, and further affected by refraction along the ray path. As a result, the final visibility of planetary auroral radio emissions strongly depends on the position of the observer. The underlying electron acceleration mechanisms depending on the considered magnetosphere, understanding the overall visibility of radiated waves is important to assess the diagnostic brought by remote radio observations onto auroral and magnetospheric dynamics. This topic has been widely studied in the literature, taking advantage of space-based radio exploration, generally on a planet-by-planet basis. In this work, we present an updated view of the visibility of Saturn's kilometric radiation from the full set of Cassini/RPWS observations obtained over 2004-2017. We then review comparatively recent parallel studies of the visibility of Terrestrial kilometric radiation and of Jovian broadband kilometric, hectometric and decametric emissions. We finally discuss the implications for the search for exoplanetary auroral radio emissions.

[1] *LESIA, Observatoire de Paris, Université PSL, CNRS, Sorbonne Université, Université de Paris, Meudon, France*

[2] *Aix Marseille Université, CNRS, CNES, LAM, Marseille, France*

[3] *School of Cosmic Physics, DIAS Dunsink Observatory, Dublin Institute for Advanced Studies, Dublin, Ireland*

1 Introduction

Powerful, non-thermal, radio emissions have been ubiquitously detected from the planetary magnetospheres of the solar system which have been observed from the ground above the terrestrial ionospheric cutoff frequency of $\sim$ 10 MHz and from space below. While the Jovian decametric (DAM) emissions have been observed by various radiotelescopes between 10 and 40 MHz from the early 1950s (Burke & Franklin, 1955), the most studied emission has been the Auroral (or Terrestrial) Kilometric Radiation (AKR) at Earth, extending from a few kHz to 1 MHz, which benefited from numerous in situ space-based observations since the 1960s (Benediktov et al., 1965; Gurnett, 1974). AKR was early identified as being (mostly) R-X mode emission produced along high latitude (auroral) magnetic flux tubes at frequencies f close to the local electron cyclotron frequency f_{ce}, itself proportional to the local magnetic field amplitude. Its properties are now fairly established, in terms of spectrum, radiated power, dynamics, high degree of circular polarization (Right- and Left-Handed polarized, hereafter RH and LH, in the northern and southern magnetic hemispheres) and strongly anisotropic beaming. Wu & Lee (1979) subsequently developed the theory of the electron Cyclotron Maser Instability (CMI), able to directly amplify R-X mode waves from mildly relativistic electrons, to account for the AKR generation. This mechanism was later validated in situ by successive polar spacecraft such as Viking, Freja, Dynamic Explorer 1 and FAST (Fast Auroral SnapshoT Explorer Baumjohann & Treumann, 2022, and references therein). In the late 1970s, the Voyager exploration of the giant planets then yielded the successive detection of Hectometric (HOM) and broadband Kilometric (b-KOM) emissions at Jupiter and Kilometric Radiation at Saturn (SKR), Uranus (UKR) and Neptune (NKR). The similarity of their macroscopic properties with those of AKR led to attribute all of them to the CMI (Louarn, 1992; Zarka, 1998, and references therein). This inference was only recently confirmed in situ at Saturn with Cassini (Lamy et al., 2010; Mutel et al., 2010) and at Jupiter with Juno (Louarn et al., 2017; Louis et al., 2020) - see also Collet et al. (2023, this issue). Hereafter, we thus restrict ourselves to the Earth, Jupiter and Saturn, whose magnetic axis is additionally weakly tilted with respect to the rotation axis, whose obliquity is low ($\leq 30°$).

The convolution of the spatial distribution of radiosources with the emission beaming, further affected by wave refraction along the ray path, controls the overall visibility of the emission. The former two characteristics depend on the topology of the planetary magnetic field and on the source of free energy (CMI-unstable Electron Distribution Function, hereafter EDF, of a few keV) associated with the acceleration mechanisms prevailing at each magnetosphere. The magnetospheric dynamics at Earth is for instance governed by the interaction with the solar wind, as opposed to that prevailing at Jupiter, mostly driven by the fast planetary rotation and planet-satellite interactions, while Saturn's magnetosphere is controlled by part of/all these drivers. The auroral processes therefore strongly depend on Local Time (LT) at Earth and Saturn, and on longitude at Jupiter and Saturn (Badman et al., 2015, and references therein). More precisely, the AKR source region lies on the nightside hemisphere and peaks pre-midnight near $\sim$22 LT (Gurnett, 1974; Panchenko, 2003). It is embedded within a plasma cavity along upward-directed field-aligned (Birkeland) currents mapping to the auroral oval (Huff et al., 1988; Hilgers et al.,

1991). AKR is radiated quasi-perpendicularly to the magnetic field vector by shell-type EDF (Roux et al., 1993; Louarn & Le Quéau, 1996; Ergun et al., 2000). Still, its apparent beaming is strongly oblique and partly filled in as the result of wave refraction at the edges of the auroral cavity (Schreiber, 2006; Mutel et al., 2008; Menietti et al., 2011). The SKR sources are distributed at all LT while reaching maximal intensity in the dawn-to-noon LT quadrant instead, peaking near ∼08 LT (Cecconi et al., 2009; Lamy et al., 2009b). They are also colocated with upward-directed field-aligned currents and (partly) with the auroral oval, wich lies at slightly larger invariant latitudes than at Earth (Bunce et al., 2010; Lamy et al., 2018). SKR appears to be radiated quasi-perpendicularly at the source by shell-type EDF (Mutel et al., 2010; Lamy et al., 2010; Schippers et al., 2011). Its strongly oblique apparent beaming is suspected to result from wave refraction near the source. Investigating the SKR visibility from the morning sector at mid-latitudes, a modeling study showed that only $\leq 5\%$ of all SKR sources and radiated power was visible instantaneously (Lamy et al., 2013). Turning to Jupiter, its auroral radio emissions decompose into two main components. The Jupiter-satellite DAM sources lie along flux tubes associated with Io, Europa and Ganymede, respectively. They take the form of arc-shaped structures in the time-frequency plane lasting for a few hours (labelled A/B and C/D for northern/southern emissions, and A/C and B/D for vertex late/early arcs) which are visible for specific phases of the moon with respect to the observer, namely $\sim 50 - 120°$ (peaking near $\sim 90°$) for B and D arcs and $\sim 160 - 260°$ (peaking near $\sim 240°$) for A and C arcs (Bigg, 1964; Louis et al., 2017; Zarka et al., 2018; Louis et al., 2020; Jácome et al., 2022). The b-KOM, HOM and DAM sources unrelated to moons have been observed at all longitudes along flux tubes mapping to 15-60 Jovian radii magnetic apices, coincident with the equatorward edge of the auroral oval (Imai et al., 2019; Louis et al., 2019, and references therein) and, more frequently, with the zone of diffuse aurora (Al Saati et al., 2022; Collet et al., 2023). All those emissions display oblique beaming at the source consistent with prominent loss cone-type EDF produced by Alfvén acceleration (Hess et al., 2007, 2008; Louarn et al., 2017, 2018), with some rare cases of shell-driven CMI (Collet et al., 2023, this issue). The role of refraction near the source has been quantified by Galopeau & Boudjada (2016) which predicts a flattened emission cone. Lastly, Jupiter HOM/DAM sources appear to be more intense in average on the duskside hemisphere, and more frequent during solar wind shock interactions (Hess et al., 2014, ands references therein) - see also (Boudouma et al., 2023, this issue).

The purpose of this study is to focus on the resulting overall visibility of auroral radio emissions at Saturn (Section 2), Jupiter (Section 3) and the Earth (Section 4), taking advantage of long-term space-based radio observations of these magnetospheres from a wide variety of positions. This approach is aimed at achieving a comparative view on the most appropriate observer's location to remotely track planetary radio emitters, and to infer general implications for the rising search for exoplanets (Section 5).

2 Saturn

The investigation of SKR properties has largely benefitted from Cassini/RPWS observations over 2004-2017 (Lamy, 2017, and references therein). Its visibility was quantified by

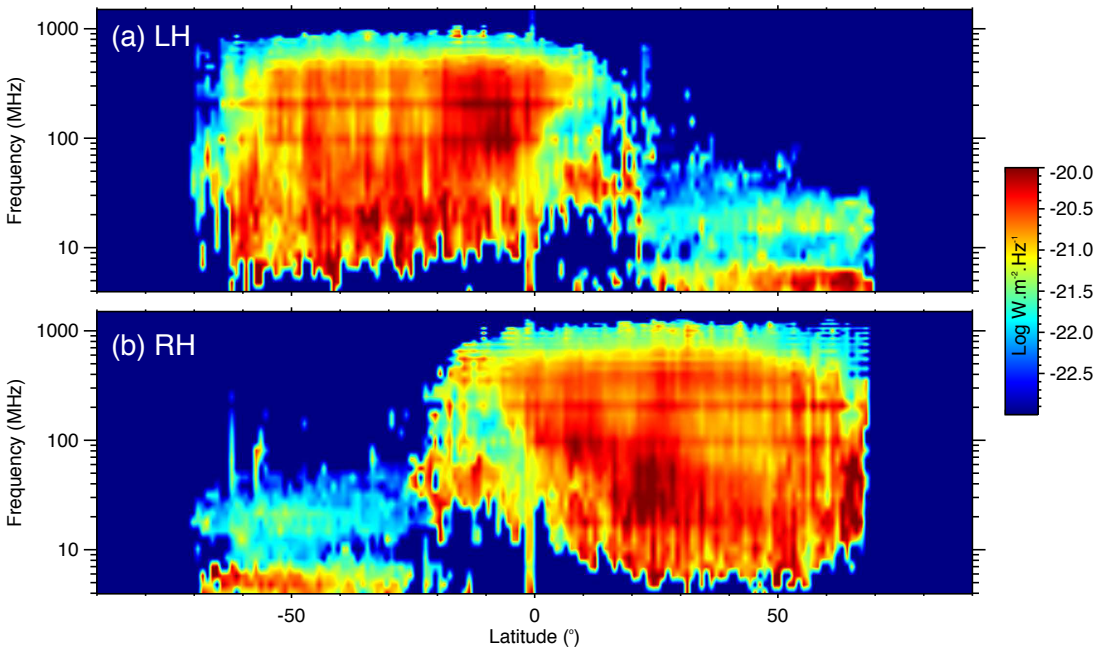

Figure 1: *Dynamic spectra of the (a) LH- and (b) RH-polarized average wave flux density normalized to 1 AU as a function of latitude, as derived from the Cassini/RPWS 2004-2017 SKR dataset. The prominent component in each hemisphere corresponds to SKR R-X mode emission. This Figure extends Figure 11 from Lamy et al. (2008a).*

building up average dynamic spectra of the wave flux density as a function of Cassini's kronocentric latitude (which roughly coincides with magnetic latitudes) and LT in the successive studies of Lamy et al. (2008a); Kimura et al. (2013); Nakamura et al. (2019), based on the same SKR data collection.

In terms of LT, the SKR spectrum was found to be more intense when observed from the morning hemisphere, with some variations depending on the considered time-interval impacted by the both the orbital geometry and the seasonal variations of the SKR activity, as illustrated in Figure 2 of Nakamura et al. (2019). When compared to the intensity profile of SKR sources mentioned in introduction, this LT distribution is broadened and smoothed, as the result of the emission visibility.

The latitudinal distribution is less affected by time-variable geometrical/seasonal effects. Figure 1 plots the SKR average flux density as a function of frequency and Cassini's latitude over the full 2004-2017 (post-orbit insertion) interval separately for both RH- and LH-polarized emissions. This Figure updates Figure 11 of Lamy et al. (2008a) which already labelled the visible components. R-X mode SKR forms the prominent emission seen in each hemisphere (RH in the north, LH in the south), with a marginal L-O mode counterpart seen near the SKR low frequency envelope in the opposite hemisphere. The two persistent bands of signal seen below $\sim 30-40$ kHz with the opposite degree of polarization correspond to narrow-banded emissions (Wu et al., 2021, and references therein). Overall, the R-X mode SKR spectrum maximizes at mid-latitudes, typically over $\sim 10-30°$ and decreases both at lower and higher latitudes. Toward the equator, the $100-500$ kHz band can be tracked down to $\sim 10-20°$ latitudes in the opposite hemi-

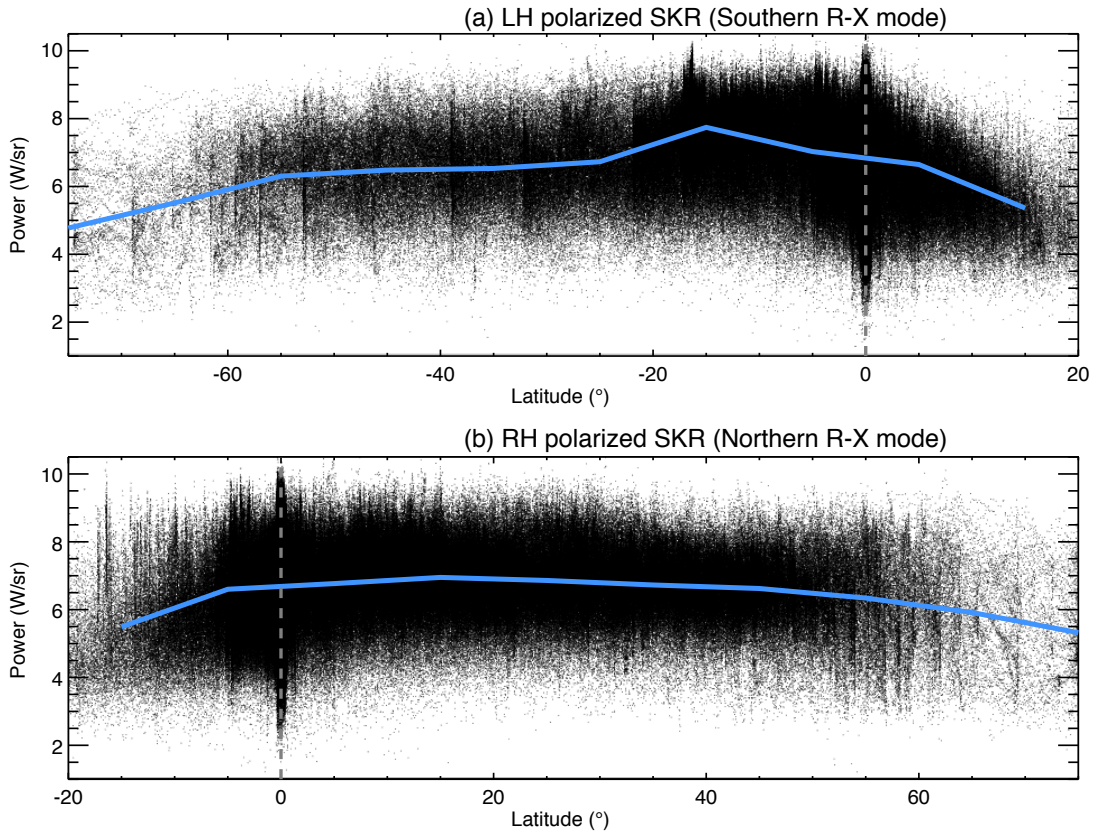

Figure 2: *(a) LH- and (b) RH-polarized wave radiated power integrated over 100-500 kHz as a function of latitude, as derived from the Cassini/RPWS 2004-2017 SKR dataset. The dots refer to individual 3-min averaged measurements. The solid blue lines draw the median behaviour of each distribution.*

sphere. Toward the pole, high and low frequencies gradually disappear beyond $\sim 50°$, respectively.

Figure 2 plots the LH- and RH-polarized radiated power integrated over 100-500 kHz, that is the peak of the SKR spectrum, as a function of latitude. The dots refer to individual 3-min averaged measurements throughout the entire 2004-2017 interval. The solid blue lines draw the median of each distribution. Those panels again show a symmetrical behavior for both hemispheres. Whatever the latitude, individual SKR measurements reveal a broad scattering extending over ≥ 6 orders of magnitude, illustrating the intrinsic variability of the emission. Both blues lines peak over $\sim 10 - 30°$. The median power measured in this range is typically $0.5 - 1$ order of magnitude larger than that signal observed from near the equator (where both hemispheres can be observed simultaneously) or from medium latitudes ($\sim 40 - 50°$). SKR was more scarcely observed beyond 60°.

3 Jupiter

Cassini/RPWS, Voyager/PRA and Nançay Decameter Array (NDA) statistical observations of Jupiter were used to produce average dynamic spectra of the full Jovian spectrum as a function of longitude (Imai et al., 2011; Zarka et al., 2021). Figure 9 of Zarka et al.

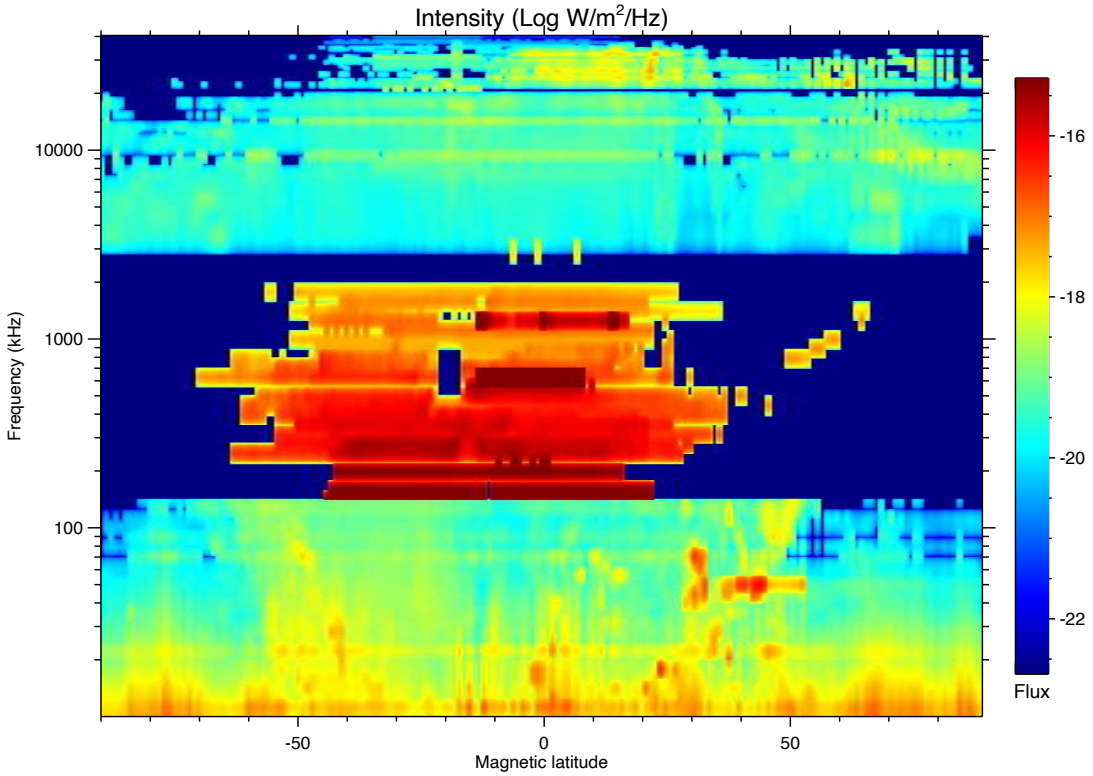

Figure 3: *Dynamic spectrum of the average wave flux density normalized to 1 AU as a function of frequency and latitude, as derived from Juno/Waves calibrated data between 2016-188 and 2019-173.*

(2021) illustrates that, altogether, the various radio components are observed from all longitudes despite some differences between RH- and LH-polarized emissions depending on the relative orientation of the magnetic dipole. As reminded in introduction, the DAM emissions induced by Io, Europa and Ganymede are visible for two specific phases windows at $\sim 40-130°$ and $\sim 150-280°$, hence near quadrature.

Taking advantage of Juno/Waves observations acquired since 2016 along polar orbits, Louis et al. (2021b) built up dynamic spectra by component as a function of magnetic latitude (see their Figure 4). The Io-DAM spectrum for instance maximizes whenever observed over $\sim 5-30°$ in each hemisphere (despite Juno/Waves cannot measure the wave polarization, northern Io-DAM arcs reach in average higher maximal frequencies than southern ones). Taken altogether, the spectrum of non-Io HOM/DAM emissions (≥ 3 MHz) also maximizes over $0-30°$ with intense emissions seen up to 80°, despite a modest hemispheric asymmetry. Interestingly, a high frequency extinction (reminiscent of that observed for SKR) is visible at high enough latitudes, and is best seen in the south below $-50°$. At lowest frequencies, the b-KOM spectrum maximizes within $10-40°$.

Figure 3 provides a compiled view of Figure 4 of Louis et al. (2021b) over the full spectral range of Juno/Waves, including the strongly attenuated band 150 kHz−3 MHz covered by the HFR-Low filter unshown before. The red color of HOM emissions seen with HFR-Low simply results from the higher background/least sensitivity of the receiver which could only track powerful enough emissions detected close enough from Jupiter, visible between $-50°$ and $+30°$ latitude.

4 Earth

Analyzing 10 years of Wind/Waves observations of AKR at Earth, Waters et al. (2022) recently statistically investigated the AKR visibility as a function of LT. Figure 4 is a modified version of their Figure 1, which displays the AKR radiated power integrated over its full 30-650 kHz spectrum as a function of LT and magnetic latitude (a fair portion of which was explored by the Wind spacecraft during the early stages of the mission). This Figure illustrates that AKR power maximizes whenever observed from the nightside and from mid-latitudes beyond 5°. The missing high latitude coverage is dealt with in a parallel analysis of POLAR radio observations (Louis et al., 2023, this issue).

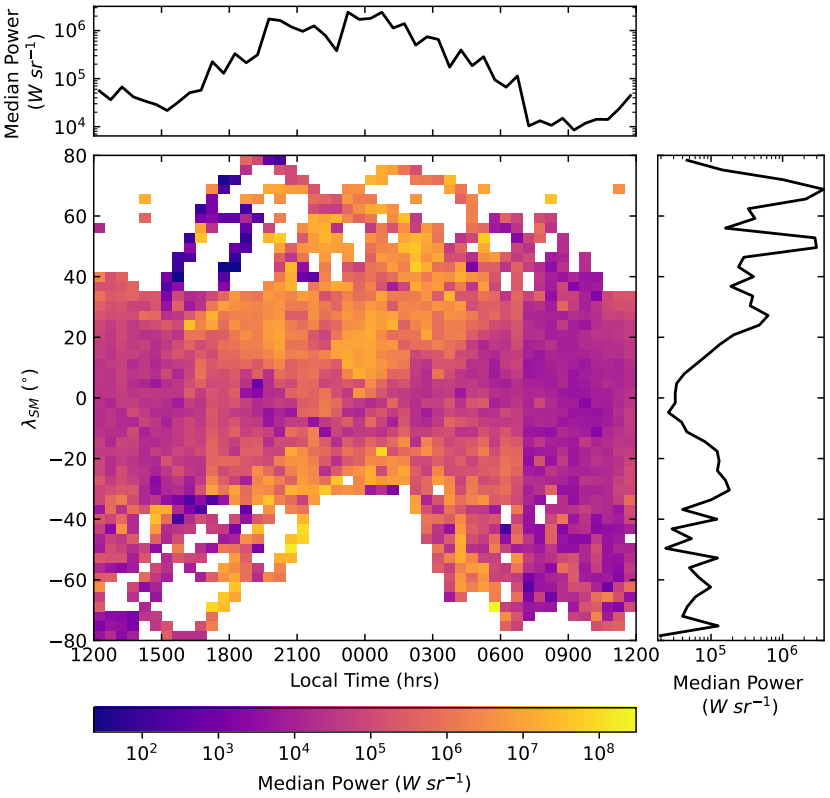

Figure 4: *Average AKR radiated power integrated over 30-650 kHz as a function of LT and magnetic latitude, as derived from Wind/Waves AKR observations from 1995 to 2004. The top and left-hand plots display the median power as a function of LT and magnetic latitude, respectively. Adapted from Waters et al. (2022).*

5 Implications for exoplanets

The universal character of the CMI was early thought to apply to a wider range of astrophysical objects (Treumann, 2006) and motivated an intense activity of the community to search for exoplanets at low frequencies. These efforts relied on predictions on the one hand and exploratory observations with ground-based radiotelescopes on the other hand. On the former side, one has to distinguish between magnetospheric radio emission from

the exoplanet itself (as for the Earth and the giant planets) and stellar radio emission induced by the electrodynamic interaction with a close-in orbiting exoplanet (transposing the Io-Jupiter archetype to hot Jupiters orbiting throughout the magnetic environment of the host star). Scaling laws using solar system measurements were therefore elaborated to predict the expected flux for emissions driven either internally or externally to the magnetosphere by star/planet interactions on the one hand (Zarka et al., 2017) and internally by Jupiter-like fast rotating magnetospheres on the other hand (Nichols & Milan, 2016). Such scaling laws were in turn used to prioritize the most promising targets (e.g. Grießmeier et al., 2007). While hints of a detection have been published with sensitive instruments such as LOFAR (e.g. Turner et al., 2021), a confirmed detection of an exoplanet at low frequencies is still pending. Still, the search for exoplanets remains a major objective of future low frequency radiotelescopes such as NenuFAR (Lamy et al., 2014; Zarka, 2020) and, ultimately, SKA-Low (Zarka et al., 2015).

The results presented in previous sections suggest that the auroral radio visibility may help to search for exoplanets by improving their "figure of merit" or conversely help to interpret validated detections. As sketched in Figure 5a, the auroral radio emissions of the Earth, Jupiter and Saturn are mostly beamed toward medium magnetic latitudes, both hemispheres illuminating the equator with a modest decrease of power. Assuming that a similar small tilt between the magnetic and the rotation axis and low obliquity of the latter prevail for distant stellar systems, observing exoplanets which transit ahead of their star ensure the observer to observe from medium latitudes, with significant chances to detect both hemispheres (either simultaneously or in alternance depending on the tilt of the rotation axis and on the rotation period).

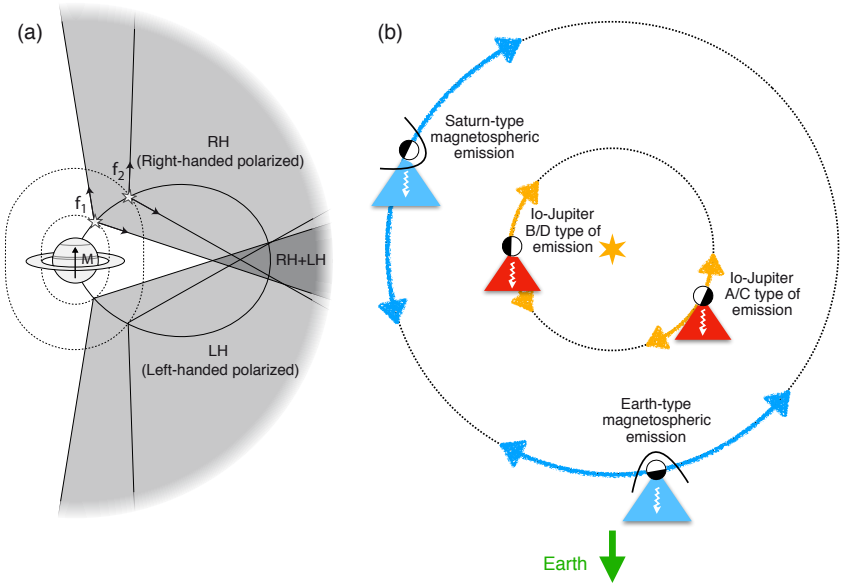

Figure 5: *Sketch of the visibility of auroral radio emissions from the Earth, Jupiter and Saturn. (a) Meridian plane showing the hemispheric beaming as a function of latitude for two frequencies f_1 and f_2 with $f_1 \geq f_2$. Both hemispheres can only be observed together from near the magnetic equator. Adapted from Lamy et al. (2008b). (b) Orbital plane of a stellar system for a terrestrial observer located at the bottom. The double arrows indicate the suitable portions of exoplanetary orbits to detect Saturn- and Earth-type of magnetospheric radio emissions (blue) and Io-Jupiter type of radio emissions (orange).*

Whenever observed from such medium latitudes, the solar system radio sources are best visible for certain phases with respect to the observer, as illustrated in Figure 5b. The Io-Jupiter arcs are detected near both quadratures, with a slight asymmetry in phase resulting from physical parameters of the Io-Jupiter interaction, such as a complex magnetic topology affecting the beaming or the presence of a dense Io plasma torus moving the Io active flux tube ahead of the position of the moon. Tracking Star-planet interactions transposing the Io-Jupiter case should similarly maximize detection near both quadratures. Interestingly, such a signature has recently been reported from GHz observations for at least two systems : Proxima Centauri (Pérez-Torres et al., 2021) and YZ Ceti (Pineda & Villadsen, 2023). The search for emission from exoplanetary magnetospheres relates to the main driver of the magnetospheric dynamics. For Earth-like magnetospheres highly sensitive to the stellar wind, the maximal chance of detection will be achieved for observations from the nightside, when the exoplanet transits or lies near inferior conjunction. Searching for Saturn-type magnetospheres, fastly rotating but with a modest enough magnetic field preserving the driving role of the stellar wind, would require observations from the morning sector, hence in quadrature. Finally, the observation of Jovian-type magnetospheres, strongly magnetized and fastly rotating, do not require any preferred position of observation (at the exception of brief transits at opposition which may yield occultation by the star).

6 Conclusions and perspectives

In this contribution, we have presented recent results on the visibility of auroral radio emissions from the Earth, Saturn and Jupiter, taking advantage of long-term space-based radio exploration of these magnetospheres from a wide variety of positions. We showed in particular that, despite some differences of secondary order, these radio emissions are mainly beamed toward their hemisphere or origin, with maximal spectra and intensities observed from medium magnetic latitudes. When investigated as a function of LT or longitude, the radio visibility significantly changes with the concerned planet depending on the primary drivers of the magnetospheric dynamics. These results illustrate that the tracking of solar system auroral radio emissions requires a suitably located observer and that an absence of detection does not imply that a low radio activity. Accounting for these visibility effects in turn needs a careful modeling of auroral radio sources. These results also provide a novel framework to the search for and/or the interpretation of auroral radio emissions from exoplanets, which stands a major objective of giant radiotelescopes in operation or under construction.

7 Acknowledgements:

The authors acknowledge support from CNES and from CNRS/INSU programs of Planetology (PNP) and Heliophysics (PNST). The Cassini/RPWS and Juno/Waves raw data are accessible through the Planetary Data System at `https://pds-ppi.igpp.ucla.edu/`, where there are referenced as Kurth & Piker (2014); Kurth et al. (2023). The

Cassini/RPWS/HFR processed data used to build Figures 1-2 are available though the LESIA-Kronos database at `https://lesia.obspm.fr/kronos/`, these consist of the SKR data collection referenced as Lamy et al. (2009a). The Juno/Waves flux calibrated data used to build Figure 3 are available though the MASER service `https://maser.obspm.fr/` and referenced as Louis et al. (2021a). The authors acknowledge support from the Wind/Waves team and CDPP for the provision of Wind/Waves RAD1 L2 data and from Paris Astronomical Data Centre (PADC) for the preparation and distribution of the data collection. The Wind/Waves/RAD1 dataset used to build Figure 4 was processed as described in Waters et al. (2021). C. K. Louis' work at the Dublin Institute for Advanced Studies was funded by the Science Foundation Ireland Grant 18/FRL/6199.

References

Al Saati S., et al., 2022, Magnetosphere-Ionosphere-Thermosphere Coupling Study at Jupiter Based on Juno's First 30 Orbits and Modeling Tools, *Journal of Geophysical Research (Space Physics)*, *127, e2022JA030586*

Badman S. V., Branduardi-Raymont G., Galand M., Hess S. L. G., Krupp N., Lamy L., Melin H., Tao C., 2015, Auroral Processes at the Giant Planets: Energy Deposition, Emission Mechanisms, Morphology and Spectra, *Space Science Reviews*, *187, 99*

Baumjohann W., Treumann R. A., 2022, Auroral kilometric radiation - The electron cyclotron maser paradigm, *Frontiers in Astronomy and Space Sciences*, *9, 1053303*

Benediktov E. A., Getmantsev G. G., Sazonov Y. A., Tarasov A. F., 1965, Preliminary results of measurements of the intensity of distributed extraterrestrial radio frequency emission at 725 and 1525 kHz frequency by the satellite Electron-2, *Kosm. Issled.*, *3*

Bigg E. K., 1964, Influence of the Satellite Io on Jupiter's Decametric Emission, *Nature*, *203, 1008*

Boudouma A., Zarka P., Magalhães F. P., Marques M. S., Louis C. K., Echer E., Lamy L., Prangé R., 2023, Localisation of the main HOM source in the dusk side of the Jovian magnetosphere, *in Planetary, Solar and Heliospheric Radio Emissions IX, eds Louis, C. K. and Jackman, C. M. and Fischer, G. and Sulaiman, A. H. and Zucca, P.*, DIAS and TCD, doi:10.25546/103094

Bunce E. J., et al., 2010, Extraordinary field-aligned current signatures in Saturn's high-latitude magnetosphere: Analysis of Cassini data during Revolution 89, *Journal of Geophysical Research (Space Physics)*, *115, A10238*

Burke B. F., Franklin K. L., 1955, Observations of a Variable Radio Source Associated with the Planet Jupiter, *Journal of Geophysical Research*, *60, 213*

Cecconi B., Lamy L., Zarka P., Prangé R., Kurth W. S., Louarn P., 2009, Goniopolarimetric study of the revolution 29 perikrone using the Cassini Radio and Plasma Wave Science instrument high-frequency radio receiver, *Journal of Geophysical Research (Space Physics)*, *114, A03215*

Collet B., Lamy L., Louis C. K., Zarka P., Prangé P., Louarn P., Sulaiman A., Kurth W. S. K., 2023, Characterization of Jovian hectometric sources with Juno: statistical position and generation by shell-type electrons, *in Planetary, Solar and Heliospheric Radio Emissions IX, eds Louis, C. K. and Jackman, C. M. and Fischer, G. and Sulaiman, A. H. and Zucca, P.*, DIAS and TCD, doi:10.25546/103095

Ergun R. E., Carlson C. W., McFadden J. P., Delory G. T., Strangeway R. J., Pritchett P. L., 2000, Electron-Cyclotron Maser Driven by Charged-Particle Acceleration from Magnetic Field-aligned Electric Fields, *Astrophysical Journal*, *538, 456*

Galopeau P. H. M., Boudjada M. Y., 2016, An oblate beaming cone for Io-controlled Jovian decameter emission, *Journal of Geophysical Research (Space Physics)*, *121, 3120*

Grießmeier J. M., Zarka P., Spreeuw H., 2007, Predicting low-frequency radio fluxes of known extrasolar planets, *Astronomy & Astrophysics*, *475, 359*

Gurnett D. A., 1974, The Earth as a radio source: Terrestrial kilometric radiation, *Journal of Geophysical Research*, *79, 4227*

Hess S., Mottez F., Zarka P., 2007, Jovian S burst generation by Alfvén waves, *Journal of Geophysical Research (Space Physics)*, *112, A11212*

Hess S., Cecconi B., Zarka P., 2008, Modeling of Io-Jupiter decameter arcs, emission beaming and energy source, *Geophysical Research Letters*, *35, L13107*

Hess S. L. G., Echer E., Zarka P., Lamy L., Delamere P. A., 2014, Multi-instrument study of the Jovian radio emissions triggered by solar wind shocks and inferred magnetospheric subcorotation rates, *Planetary and Space Science*, *99, 136*

Hilgers A., Roux A., Lundin R., 1991, Characteristics of AKR sources; A statistical description, *Geophysical Research Letters*, *18, 1493*

Huff R. L., Calvert W., Craven J. D., Frank L. A., Gurnett D. A., 1988, Mapping of auroral kilometric radiation sources to the aurora, *Journal of Geophysical Research*, *93, 11445*

Imai M., Imai K., Higgins C. A., Thieman J. R., 2011, Comparison between Cassini and Voyager observations of Jupiter's decametric and hectometric radio emissions, *Journal of Geophysical Research (Space Physics)*, *116, A12233*

Imai M., Greathouse T. K., Kurth W. S., Gladstone G. R., Louis C. K., Zarka P., Bolton S. J., Connerney J. E. P., 2019, Probing Jovian Broadband Kilometric Radio Sources Tied to the Ultraviolet Main Auroral Oval With Juno, *Geophysical Research Letters*, *46, 571*

Jácome H. R. P., Marques M. S., Zarka P., Echer E., Lamy L., Louis C. K., 2022, Search for Jovian decametric emission induced by Europa on the extensive Nançay Decameter Array catalog, *Astronomy & Astrophysics*, *665, A67*

Kimura T., et al., 2013, Long-term modulations of Saturn's auroral radio emissions by the solar wind and seasonal variations controlled by the solar ultraviolet flux, *Journal of Geophysical Research (Space Physics)*, *118, 7019*

Kurth W. S., Piker C. W., 2014, Cassini V/E/S/S/SS RPWS raw complete TLM packets V1.0, CO-V/E/J/S/SS-RPWS-2-REFDR-ALL-V1.0 [dataset], doi:10.17189/1519614

Kurth W. S., Robison W. T., Granroth L. J., 2023, Juno E/J/S/SS Waves Calibrated Survey Full Resolution V1.0, NO-E/J/SS-WAV-3-CDR-SRVFULL-V1.0 [dataset], doi:10.17189/1520498

Lamy L., 2017, The Saturnian kilometric radiation before the Cassini Grand Finale, *in Planetary Radio Emissions VIII, eds Fischer, G. and Mann, G. and Panchenko, M. and Zarka, P.*, pp 171–190, doi:10.1553/PRE8s171

Lamy L., Zarka P., Cecconi B., Prangé R., Kurth W. S., Gurnett D. A., 2008a, Saturn kilometric radiation: Average and statistical properties, *Journal of Geophysical Research (Space Physics)*, *113, A07201*

Lamy L., Zarka P., Cecconi B., Prangé R., Kurth W. S., Gurnett D. A., 2008b, Saturn kilometric radiation: Average and statistical properties, *Journal of Geophysical Research (Space Physics)*, *113, A07201*

Lamy L., Cecconi B., Zarka P., 2009a, Cassini/RPWS/HFR LESIA/Kronos SKR Data Collection, doi:10.25935/ZKXB-6C84, `https://doi.org/10.25935/ZKXB-6C84`

Lamy L., Cecconi B., Prangé R., Zarka P., Nichols J. D., Clarke J. T., 2009b, An auroral oval at the footprint of Saturn's kilometric radio sources, colocated with the UV aurorae, *Journal of Geophysical Research (Space Physics)*, *114, A10212*

Lamy L., et al., 2010, Properties of Saturn kilometric radiation measured within its source region, *Geophysical Research Letters*, *37, L12104*

Lamy L., et al., 2013, Multispectral simultaneous diagnosis of Saturn's aurorae throughout a planetary rotation, *Journal of Geophysical Research (Space Physics)*, *118, 4817*

Lamy L., Griessmeier J.-M., Zarka P., Girard J., Hess S. L. G., 2014, Search for exoplanetary radio emissions with NenuFAR, *in The NenuFAR science case, eds Zarka, P. and Tagger, M.*, pp 98–106, doi:10.5281/zenodo.8056398

Lamy L., et al., 2018, The low-frequency source of Saturn's kilometric radiation, *Science*, *362, aat2027*

Louarn P., 1992, Auroral planetary radio emissions, theoretical aspects, *Advances in Space Research*, *12, 121*

Louarn P., Le Quéau D., 1996, Generation of the Auroral Kilometric Radiation in plasma cavities - II. The cyclotron maser instability in small size sources, *Planetary and Space Science*, *44, 211*

Louarn P., et al., 2017, Generation of the Jovian hectometric radiation: First lessons from Juno, *Geophysical Research Letters*, *44, 4439*

Louarn P., et al., 2018, Observation of Electron Conics by Juno: Implications for Radio Generation and Acceleration Processes, *Geophysical Research Letters*, *45, 9408*

Louis C. K., Lamy L., Zarka P., Cecconi B., Hess S. L. G., 2017, Detection of Jupiter decametric emissions controlled by Europa and Ganymede with Voyager/PRA and Cassini/RPWS, *Journal of Geophysical Research (Space Physics)*, *122, 9228*

Louis C. K., Prangé R., Lamy L., Zarka P., Imai M., Kurth W. S., Connerney J. E. P., 2019, Jovian Auroral Radio Sources Detected In Situ by Juno/Waves: Comparisons With Model Auroral Ovals and Simultaneous HST FUV Images, *Geophysical Research Letters*, *46, 11,606*

Louis C. K., Louarn P., Allegrini F., Kurth W. S., Szalay J. R., 2020, Ganymede-Induced Decametric Radio Emission: In Situ Observations and Measurements by Juno, *Geophysical Research Letters*, *47, e90021*

Louis C. K., Zarka P., Cecconi B., 2021a, Juno/Waves estimated flux density Collection (Version 1.0), doi:10.25935/6jg4-mk86

Louis C. K., Zarka P., Dabidin K., Lampson P. A., Magalhães F. P., Boudouma A., Marques M. S., Cecconi B., 2021b, Latitudinal Beaming of Jupiter's Radio Emissions From Juno/Waves Flux Density Measurements, *Journal of Geophysical Research (Space Physics)*, *126, e29435*

Louis C. K., Smith K. D., Jackman C. M., Fogg A. R., Waters J. E., O'Dwyer E. P., Granroth L., 2023, Latitudinal distribution of auroral kilometric radiation based on Polar spacecraft observations, *in Planetary, Solar and Heliospheric Radio Emissions IX, eds Louis, C. K. and Jackman, C. M. and Fischer, G. and Sulaiman, A. H. and Zucca, P.*, DIAS and TCD, doi:10.25546/103088

Menietti J. D., Mutel R. L., Christopher I. W., Hutchinson K. A., Sigwarth J. B., 2011, Simultaneous radio and optical observations of auroral structures: Implications for AKR beaming, *Journal of Geophysical Research (Space Physics)*, *116, A12219*

Mutel R. L., Christopher I. W., Pickett J. S., 2008, Cluster multispacecraft determination of AKR angular beaming, *Geophysical Research Letters*, *35, L07104*

Mutel R. L., et al., 2010, CMI growth rates for Saturnian kilometric radiation, *Geophysical Research Letters*, *37, L19105*

Nakamura Y., et al., 2019, Seasonal variation of north-south asymmetry in the intensity of Saturn Kilometric Radiation from 2004 to 2017, *Planetary and Space Science*, *178, 104711*

Nichols J. D., Milan S. E., 2016, Stellar wind-magnetosphere interaction at exoplanets: computations of auroral radio powers, *Monthly Notices of the RAS*, *461, 2353*

Panchenko M., 2003, Direction finding of AKR sources with three orthogonal antennas, *Radio Science*, *38, 1099*

Pérez-Torres M., et al., 2021, Monitoring the radio emission of Proxima Centauri, *Astronomy & Astrophysics*, *645, A77*

Pineda J. S., Villadsen J., 2023, Coherent radio bursts from known M-dwarf planet-host YZ Ceti, *Nature Astronomy*, *7, 569*

Roux A., et al., 1993, Auroral kilometric radiation sources: In situ and remote observations from Viking, *Journal of Geophysical Research*, *98, 11657*

Schippers P., et al., 2011, Auroral electron distributions within and close to the Saturn kilometric radiation source region, *Journal of Geophysical Research (Space Physics)*, *116, A05203*

Schreiber R., 2006, Partially Filled AKR Emission Cones, *in Planetary Radio Emissions VI*, pp 249–255

Treumann R. A., 2006, The electron-cyclotron maser for astrophysical application, *Astronomy & Astrophysics Reviews*, *13, 229*

Turner J. D., et al., 2021, The search for radio emission from the exoplanetary systems 55 Cancri, υ Andromedae, and τ Boötis using LOFAR beam-formed observations, *Astronomy & Astrophysics*, *645, A59*

Waters J. E., Jackman C. M., Lamy L., Cecconi B., Whiter D. K., Bonnin X., Issautier K., Fogg A. R., 2021, Empirical Selection of Auroral Kilometric Radiation During a Multipoint Remote Observation With Wind and Cassini, *Journal of Geophysical Research (Space Physics)*, *126, e29425*

Waters J. E., et al., 2022, A Perspective on Substorm Dynamics Using 10 Years of Auroral Kilometric Radiation Observations From Wind, *Journal of Geophysical Research (Space Physics)*, *127, e30449*

Wu C. S., Lee L. C., 1979, A theory of the terrestrial kilometric radiation., *Astrophysical Journal*, *230, 621*

Wu S., Ye S., Fischer G., Wang J., Long M., Menietti J. D., Cecconi B., Kurth W. S., 2021, Statistical Study on Spatial Distribution and Polarization of Saturn Narrowband Emissions, *Astrophysical Journal*, *918, 64*

Zarka P., 1998, Auroral radio emissions at the outer planets: Observations and theories, *Journal of Geophysical Research*, *103, 20159*

Zarka P. e. a., 2020, The low-frequency radio telescope NenuFAR, *in Proceedings of the URSI GASS 2020 conference hold in Rome 29/8-5/9/2020*, pp 1–4

Zarka P., Lazio J., Hallinan G., 2015, Magnetospheric Radio Emissions from Exoplanets with the SKA, *in Advancing Astrophysics with the Square Kilometre Array (AASKA14)*, p. 120, doi:10.22323/1.215.0120

Zarka P., et al., 2017, Radio emission from the Ganymede-Jupiter interaction and consequence for radio emissions from exoplanets, *in Radio Exploration of Planetary Habitability (AASTCS5)*, p. 202.04

Zarka P., Marques M. S., Louis C., Ryabov V. B., Lamy L., Echer E., Cecconi B., 2018, Jupiter radio emission induced by Ganymede and consequences for the radio detection of exoplanets, *Astronomy & Astrophysics*, *618, A84*

Zarka P., Magalhães F. P., Marques M. S., Louis C. K., Echer E., Lamy L., Cecconi B., Prangé R., 2021, Jupiter's Auroral Radio Emissions Observed by Cassini: Rotational Versus Solar Wind Control, and Components Identification, *Journal of Geophysical Research (Space Physics)*, *126, e29780*